JOURNAL OF MOLECULAR SPECTROSCOPY 120, 421–434 (1986)

The Far-Infrared Laser Magnetic Resonance Spectrum of the CF Radical and Determination of Ground State Parameters[1]

JOHN M. BROWN

Physical Chemistry Laboratory, South Parks Road, Oxford OX1 3QZ, England

JANETTE E. SCHUBERT[2]

Department of Chemistry, University of Southampton, Southampton SO9 5NH, England

RICHARD J. SAYKALLY

Department of Chemistry, University of California, Berkeley, California 94720

AND

KENNETH M. EVENSON

National Bureau of Standards, Boulder, Colorado 80303

Observations in the far-infrared laser magnetic resonance spectrum of the CF radical in its ground $^2\Pi$ state have been extended to include fine structure transitions between the two spin components. The data are fitted together with all previous measurements relating to the $v = 0$ level to obtain a complete set of molecular parameters, including the spin-orbit splitting which has been determined at 77.196916(14) cm^{-1}. The implications for the electronic structure of various parameters are also discussed.

1. INTRODUCTION

The CF radical has been extensively studied in its ground electronic state ($X^2\Pi$) by a variety of spectroscopic techniques. It was first detected in 1950 by Andrews and Barrow (*1*) through the observation of the $A^2\Sigma^+$–$X^2\Pi$ transition in its electronic spectrum. This band system was examined along with others in considerable detail, first by Andrews and Barrow (*2*) and later by Porter *et al.* (*3*). Data were fit for several vibrational levels and it was determined that the ground state is regular. Higher precision measurements of transitions involving rotational levels of the ground state ($v = 0$) have since been made by gas phase EPR (*4*), microwave (*5*), and far-infrared spectroscopy (*6, 7*). In addition, the infrared spectrum of CF has been studied, by diode laser spectroscopy (*8*) and by carbon monoxide laser magnetic resonance (LMR) spectroscopy (*9*). Taken together these measurements provide a wealth of information about CF. Virtually all of its molecular parameters are well determined, the notable

[1] Work supported in part by NASA Contract W-15, 047.

[2] Present address: Pion Ltd., Brondesbury Park, London NW2 5JN, England.

0022-2852/86 $3.00

exception being the spin-orbit coupling constant A which is only known with fairly modest reliability (77.11 ± 0.03 cm^{-1}) from the work of Porter *et al.* (*3*) on the optical spectrum. The spin-orbit splitting in CF corresponds to a quantum in the far-infrared region of the spectrum. The observation of fine structure transitions between the $^2\Pi_{3/2}$ and $^2\Pi_{1/2}$ components allows the direct measurement of the spin-orbit coupling parameter. Such transitions are weaker than pure rotational transitions by a factor of about $(B/A)^2 \simeq 0.0003$ where B is the rotational constant (*10*) but the sensitivity of the LMR technique is quite sufficient to allow their detection (*11, 12*).

This paper describes the measurement and analysis of further far-infrared LMR spectra of CF, including three fine structure transitions. These data are combined with all the earlier measurements relating to the $v = 0$ level in a global fit to determine the best set of molecular parameters, including the spin-orbit coupling constant. The implications of these parameter values for the electronic structure of the CF radical are discussed briefly.

2. EXPERIMENTAL DETAILS

The spectra were recorded at the Boulder Laboratories of the NBS with a far-infrared LMR spectrometer which has been described in detail elsewhere (*13*). The CF radicals were produced in the spectrometer sample volume by the reaction of fluorine atoms with methane in a flow system, the fluorine atoms being generated by passing a mixture of He and F_2 through a microwave discharge (*7*). The total pressure in the sample region was about 1 Torr (133 Pa) of which only 0.1% was methane. The LMR spectrometer magnet was controlled by a rotating coil system which provided a direct readout of the flux density. The system was calibrated periodically with a proton NMR

TABLE I

Summary of Observations in the Far-Infrared LMR Spectrum of the CF Radical in the $v = 0$ Level of the $X^2\Pi$ State

Pump	Laser line Gain medium	λ/μm	ν/GHz [a]	CF transition
9R(20)	CH_2F_2	117.7	2546.4950	$F_2 \leftarrow F_1$, $J = 3\frac{1}{2} \leftarrow 2\frac{1}{2}$ [b]
				$F_2 \leftarrow F_1$, $J = 14\frac{1}{2} \leftarrow 14\frac{1}{2}$
9R(22)	CH_2F_2	122.4	2447.9685	$F_2 \leftarrow F_1$, $J = 2\frac{1}{2} \leftarrow 1\frac{1}{2}$
				$F_2 \leftarrow F_1$, $J = 11\frac{1}{2} \leftarrow 11\frac{1}{2}$
10R(24)	DCOOD	304.1	985.8897	$F_2 \leftarrow F_2$, $J = 11\frac{1}{2} \leftarrow 10\frac{1}{2}$
10R(12)	DCOOD	380.6	787.7555	$F_1 \leftarrow F_1$, $J = 9\frac{1}{2} \leftarrow 8\frac{1}{2}$
10R(8)	N_2H_4	533.6	561.7720	$F_2 \leftarrow F_2$, $J = 6\frac{1}{2} \leftarrow 5\frac{1}{2}$
10P(36)	CD_3I	556.9	538.3473	$F_1 \leftarrow F_1$, $J = 6\frac{1}{2} \leftarrow 5\frac{1}{2}$
9P(20)	CH_2CHCl	634.5	472.5077	$F_2 \leftarrow F_2$, $J = 5\frac{1}{2} \leftarrow 4\frac{1}{2}$
10R(26)	CH_2CHBr	635.4	471.8505	$F_2 \leftarrow F_2$, $J = 5\frac{1}{2} \leftarrow 4\frac{1}{2}$
9P(10)	CH_2F_2	657.2	456.1391	$F_1 \leftarrow F_1$, $J = 5\frac{1}{2} \leftarrow 4\frac{1}{2}$

[a] Frequencies given by Inguscio, Moruzzi, Evenson and Jennings (*26*).

[b] F_2 is the $^2\Pi_{\frac{3}{2}}$ spin component and F_1 the $^2\Pi_{\frac{1}{2}}$ spin component.

gaussmeter from 0.05 up to 1.8 T. A fractional uncertainty of 10^{-4} can be achieved by careful measurement for flux densities above 0.1 T. However, because of the large number of resonances involved in the spectrum of CF, a measurement to ±0.1 mT was considered acceptable in practice.

The far-infrared LMR spectrum of the CF radical in the $v = 0$ level of the $X^2\Pi$ state is summarized in Table I; this includes the observations made in the previous study (*7*). Six rotational transitions and four fine structure transitions have been identified using nine laser lines, as shown in the energy level diagram of Fig. 1. The diagram also shows the transitions studied in the tunable far-infrared experiments (*6*), the microwave spectrum (*5*), and in the EPR spectrum (*4*). The 556.9-μm spectrum of the CF radical in perpendicular polarization is reproduced in Fig. 2a. Some other representative LMR spectra were shown in the earlier paper (*7*).

3. ASSIGNMENT AND FITTING

3.1. Analysis

The LMR spectra of the CF radical were assigned with the help of a predictive computer program which has been described earlier (*14*). The rotational quantum

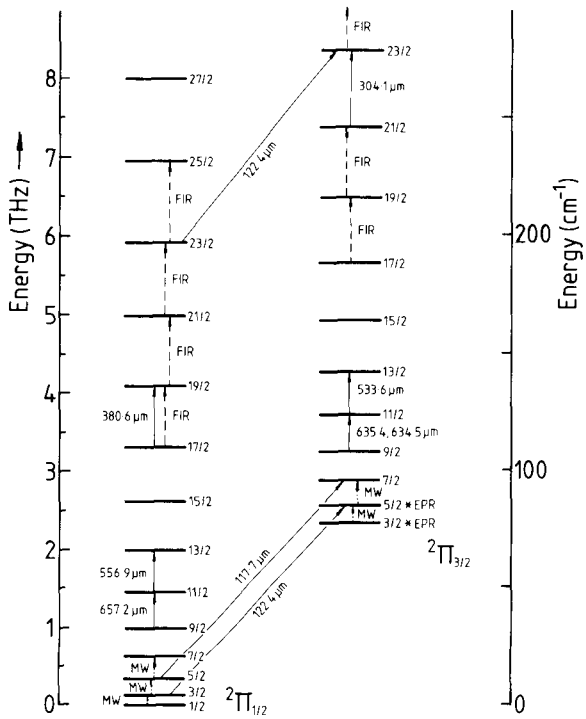

FIG. 1. Diagram showing the low-lying rotational energy levels of the CF radical in the $v = 0$ level of the $X^2\Pi$ state. The transitions involved in the observed far-infrared LMR spectrum are indicated by the appropriate laser wavelengths. The diagram also shows the transitions involved in the EPR spectrum (*4*) (marked with asterisks), the microwave spectrum (*5*), and the tunable far-infrared spectrum (*6*).

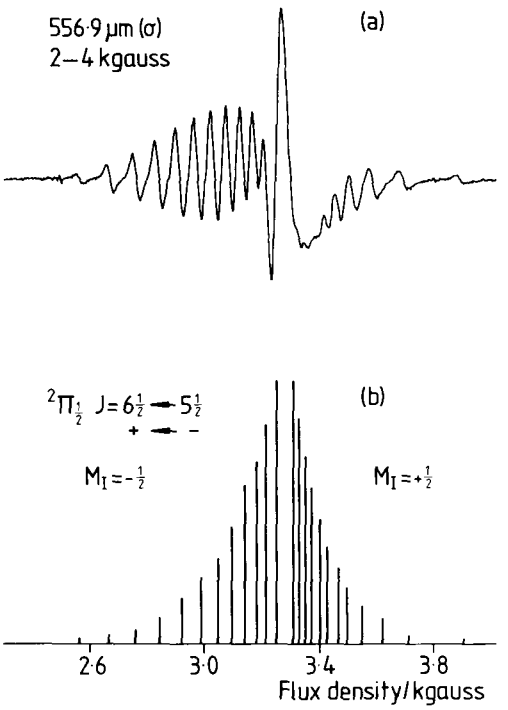

FIG. 2. Diagram showing (a) the spectrum of CF recorded with the 556.9-μm laser line in perpendicular polarization and (b) a theoretical simulation using the best fit parameters in Table IV. The transitions all follow the selection rule $\Delta M_J = +1$, $\Delta M_I = 0$; the two halves of the spectrum correspond to $M_I = -\frac{1}{2}$ and $+\frac{1}{2}$ as indicated.

numbers could be assigned simply by a comparison of the molecular transition frequency with the laser frequency. The computer program calculates all possible Zeeman transitions in an LMR spectrum above a selected intensity. With a little trial and error, it was possible to match the predictions of the computer program with the experimental spectra and thus to make the assignments directly. The LMR spectra listed in Table I represent a very large number of lines. In order to keep the data set down to a manageable size, we have selected the measurements for only four laser lines for use in the least-squares fit (117.7, 122.4, 556.9, and 635.4 μm). Full details of the experimental measurements for these spectra and their assignments are given in Table II. For the most part, the transitions obey the expected selection rule $\Delta M_J = 0$ (π polarization) or ± 1 (σ polarization) and $\Delta M_I = 0$. In addition, a number of weaker transitions which are formally forbidden ($\Delta M_I \neq 0$) are also observed at low fields where the hyperfine interaction is comparable with the Zeeman interaction.

The analysis of the remaining spectra in Table I are described in detail elsewhere (*15*). The observed Zeeman patterns can be very complicated, but in all cases they are reproduced well by calculation with the final set of molecular parameters. A simulation of the 556.9-μm spectrum is shown in Fig. 2b.

3.2. *Least-Squares Fit*

The available data for CF in the $v = 0$ level were used in a least-squares fit to determine an optimal set of molecular parameters. The data set of 179 transitions comprised:

(a) the microwave frequencies of Saito *et al.* (*5*) for the transitions $J = 3\frac{1}{2} \leftarrow 2\frac{1}{2}$, $2\frac{1}{2} \leftarrow 1\frac{1}{2}$ in both spin components and for $J = 1\frac{1}{2} \leftarrow \frac{1}{2}$ in the $^2\Pi_{1/2}$ component,

(b) the pure rotational transition frequencies of Van den Heuvel *et al.* (*6*) for $J = 9\frac{1}{2} \leftarrow 8\frac{1}{2}$, $10\frac{1}{2} \leftarrow 9\frac{1}{2}$, $12\frac{1}{2} \leftarrow 11\frac{1}{2}$ in both spin components and for $J = 11\frac{1}{2} \leftarrow 10\frac{1}{2}$ in the $^2\Pi_{1/2}$ component,

(c) the EPR data from Carrington and Howard (*4*) for the $J = 1\frac{1}{2}$ and $2\frac{1}{2}$ levels of the $^2\Pi_{3/2}$ component, and

(d) the data in the LMR spectra at 117.7, 122.4, 556.9, and 635.4 μm given in Table II.

The Hamiltonian used to model the data was formulated as a power series in $\mathbf{N}^2$ and has been described elsewhere (*14, 16*). The CF molecule in its ground state conforms well to Hund's coupling case (a) and corresponding combinations of parameters (such as $(p + 2q)$, $(A + \gamma)$, $h_{1/2}$) were determined in the fit. Since it is not possible to determine both the parameters A_D and γ in a fit of a single species in a $^2\Pi$ state, we have performed the fit with the former constrained to zero. Consequently, the parameters determined as A and γ take effective values, denoted by a tilde (e.g., $\tilde{A}$) in our results. The basis set was truncated at $\Delta J = \pm 1$ for the most part and at $\Delta J = \pm 2$ for the high field magnetic resonance lines. These limits were determined by trial calculations not to restrict the accuracy of the results. Each datum was weighted in the fit inversely as the square of the experimental error (*5, 6*). The weights are given for the LMR measurements in Table II; the main contribution to the error comes from the uncertainty in the knowledge of the far-infrared laser frequencies ($\sim 5 \times 10^{-7}$). It appeared from both our own fits of the microwave frequencies and that published by Saito *et al.* (*5*) that the author's estimate of the experimental uncertainty was too small for these measurements. In our final fit, most of the microwave frequencies were therefore assigned a weight of 400 MHz^{-2}, corresponding to an uncertainty of ± 0.05 MHz. Full details of the weightings adopted for the zero field data are given in Table III.

Five of the parameters in the model Hamiltonian were constrained to calculated values in the fit. Only one of these is a major parameter, namely the electron spin g-factor g_S which was fixed at a relativistically corrected value of 2.00196 (*7*). The other four were estimated from the following formulae:

$$H_0 \simeq H_e = \tfrac{2}{3} D_e[12(B_e/\omega_e)^2 - \alpha_e/\omega_e], \tag{1}$$

$$q_D = -4Dq/B, \tag{2}$$

$$g_l' = p/2B, \tag{3}$$

and

$$g_r e' = -q/B. \tag{4}$$

TABLE II

Observed Lines in Magnetic Resonance Spectra of the CF Radical in Its Ground State

Lower state parity	M_J'	M_J'' [a]	M_I [b]	Flux density (mT)	Obs-Calc (MHz)	Wt [c] $(MHz)^{-2}$
635.4 μm (ν_L = 471850.5 MHz) F_2, J = 5½ ← F_2, J = 4½						
Parallel polarization (π)						
+	4½	4½	½	302.83	0.1	1.0
-	4½	4½	½	306.65	0.2	1.0
+	4½	4½	-½	334.50	0.7	1.0
-	4½	4½	-½	339.34	0.8	1.0
+	3½	3½	½	396.29	0.2	1.0
-	3½	3½	½	401.58	0.4	1.0
+	3½	3½	-½	424.24	0.7	1.0
-	3½	3½	-½	430.31	0.9	1.0
+	2½	2½	½	559.84	0.3	1.0
-	2½	2½	½	567.38	0.4	1.0
+	2½	2½	-½	585.95	0.5	1.0
-	2½	2½	-½	594.20	0.8	1.0
+	1½	1½	½	930.90	0.4	1.0
-	1½	1½	½	943.43	0.5	1.0
+	1½	1½	-½	956.11	0.5	1.0
-	1½	1½	-½	969.10	0.6	1.0
Perpendicular polarization (σ)						
+	3½	4½	½	228.17	-0.2	1.0
-	3½	4½	½	230.28	-0.1	1.0
+	3½	4½	-½	266.43	1.4	1.0
-	3½	4½	-½	270.72	1.5	1.0
+	2½	3½	½	285.05	0.4	1.0
-	2½	3½	½	288.34	0.6	1.0
+	2½	3½	-½	317.22	1.4	1.0
-	2½	3½	-½	322.21	1.5	1.0
+	1½	2½	½	366.30	0.7	1.0
-	1½	2½	½	370.73	0.8	1.0
+	1½	2½	-½	396.28	1.3	1.0
+	5½	4½	½	433.15	-0.1	1.0
-	5½	4½	½	439.94	-0.0	1.0
+	5½	4½	-½	463.19	-0.3	1.0
-	5½	4½	-½	458.69	-0.1	1.0
+	½	1½	½	502.97	0.8	1.0
-	½	1½	½	509.30	1.0	1.0
+	½	1½	-½	532.57	1.4	1.0
-	½	1½	-½	540.81	1.6	1.0
+	4½	3½	½	628.00	-0.5	1.0
-	4½	3½	½	637.30	-0.2	1.0
+	4½	3½	-½	646.16	-0.5	1.0
-	4½	3½	-½	653.89	-0.4	1.0
+	-½	½	½	787.34	1.5	1.0
-	-½	½	½	797.93	2.1	1.0
+	-½	½	-½	814.80	-1.5	1.0
-	-½	½	-½	831.01	2.1	1.0
+	3½	2½	½	1113.79	-1.2	1.0
-	3½	2½	½	1128.46	-1.5	1.0
+	3½	2½	-½	1128.46	-0.9	1.0
-	3½	2½	-½	1140.40	-1.4	1.0

[a] Refers to lower state.

[b] Unless indicated, the transitions obeyed the selection rule $\Delta M_I = 0$.

[c] See test for a discussion of the weighting factors in the least-squares fit.

TABLE II—*Continued*

Lower State parity	M_J'	M_J'' [a]	M_I [b]	Flux density (mT)	Obs-Calc (MHz)	Wt [c] $(MHz)^{-2}$
	556.9 μm (ν_L = 538347.0 MHz) F_1, J = 6½ ← F_1, J = 5½					
Parallel polarization (π)						
-	-6½	-5½	½←-½	278.92	2.1	1.0
+	5½	5½	½	1222.37.	2.0	1.0
Perpendicular polarization (σ)						
-	-3½	-4½	-½	261.91	1.7	1.0
-	-2½	-3½	-½	272.44	1.5	1.0
-	-1½	-2½	-½	281.28	1.5	1.0
-	-½	-1½	-½	288.85	1.5	1.0
-	½	-½	-½	288.90	5.3	1.0
-	1½	½	-½	295.59	4.9	1.0
-	2½	1½	-½	307.20	1.6	1.0
-	3½	2½	-½	312.30	1.6	1.0
-	4½	3½	-½	316.91	1.6	1.0
-	5½	4½	-½	321.44	1.4	1.0
-	-½	-1½	½	349.12	2.1	1.0
-	-1½	-2½	½	354.04	1.5	1.0
-	-2½	-3½	½	360.93	1.4	1.0
-	-3½	-4½	½	371.21	1.4	1.0
-	-4½	-5½	½	389.76	1.6	1.0
	122.4 μm (ν_L = 2447968.5 MHz) F_2, J = 2½ ← F_1, J = 1½					
Parallel polarization (π)						
+	-1½	-½	½←-½	169.4	-3.4	0.334
+	-1½	-1½	-½	215.9	0.0	0.334
-	-1½	-½	½←-½	280.3	0.4	0.334
+	-1½	-1½	½	285.6	-0.5	0.334
-	-1½	-1½	½	312.4	0.1	0.334
-	-1½	-1½	-½	360.3	-1.8	0.334
+	-½	½	½←-½	523.9	0.8	0.334
+	-½	-½	-½	677,5	-1.8	0.334
Perpendicular polarization (σ)						
+	-2½	-1½	-½	127.5	-2.3	0.334
-	-2½	-1½	½	156.9	-6.6	0.334
+	-2½	-1½	½	158.5	-6.5	0.334
+	-1½	½	½	161.0	-3.6	0.334
-	-2½	-½	½←-½	175.1	-7.6	0.334
+	-1½	-½	-½	204.55	0.4	0.334
-	-2½	-1½	-½	209.8	-1.0	0.334
-	-1½	½	½←-½	255.3	-3.0	0.334
+	-1½	-½	½	260.9	-3.2	0.334
-	-1½	-½	½	294.8	-4.6	0.334
+	-1½	-1½	-½ ← ½	320.5	0.1	0.334
-	-1½	-1½	-½ ← ½	346.4	-0.4	0.334
+	-½	½	½	459.0	2.8	0.334

The values used for these parameters in the final fit are given in Table IV. The two terms in square brackets in Eq. (1) accidentally cancel each other, resulting in a very small (insignificant) value for H_0 of -0.73×10^{-9} MHz.

The results of the fit are given in Table II for the LMR data and in Table III for

TABLE II—*Continued*

Lower state parity	M_J'	M_J'' [a]	M_I [b]	Flux density (mT)	Obs-Calc (MHz)	Wt [c] $(MHz)^{-2}$
	122.4 μm F_2, J = 11½ ← F_1, J = 11½					
Parallel polarization (π)						
+	-11½	-11½	½	350.7	-1.0	0.334
+	-10½	-10½	½	384.2	0.5	0.334
+	-9½	-10½	-½←½	391.6	0.9	0.334
+	-11½	-11½	-½	406.9	0.3	0.334
+	-9½	-9½	½	425.3	-1.8	0.334
+	-10½	-10½	-½	444.0	1.2	0.334
+	-8½	-8½	½	475.3	0.0	0.334
+	-9½	-9½	-½	488.3	3.5	0.334
+	-7½	-7½	½	539.2	-2.5	0.334
+	-8½	-8½	-½	543.5	-0.6	0.334
+	-7½	-8½	½←-½	611.8	-1.3	0.334
+	-6½	-6½	½	621.6	-2.5	0.334
+	-6½	-6½	-½	699.2	-0.8	0.334
Perpendicular polarization (σ)						
+	-8½	-9½	½	437.7	0.9	0.334
+	-7½	-8½	½	490.9	2.4	0.334
+	-8½	-7½	½	519.5	0.6	0.334
+	-9½	-8½	-½	525.8	3.6	0.334
	117.7 μm (ν_L = 2546495.0 MHz) F_2, J = 3½ ← F_1, J = 2½					
Perpendicular polarization (σ)						
+	3½	2½	½	385.65	5.0	0.308
+	3½	2½	-½	455.6	2.4	0.308
-	3½	2½	-½	492.4	3.1	0.308
+	2½	½	-½←½	505.5	3.0	0.308
+	2½	1½	½	530.7	3.0	0.308
-	3½	1½	-½←½	556.5	3.4	0.308
-	3½	2½	½	558.5	4.7	0.308
+	2½	1½	-½	598.2	3.1	0.308
-	2½	½	-½←½	634.3	2.7	0.308
-	2½	1½	½	691.8	4.1	0.308
-	2½	1½	-½	744.05	1.5	0.308
-	2½	2½	½←-½	782.5	3.8	0.308
+	1½	½	½	821.9	1.2	0.308
+	1½	½	-½	878.6	1.9	0.308
-	1½	½	½	1042.5	-0.1	0.308
-	1½	½	-½	1114.3	-1.6	0.308
EPR SPECTRUM (ν = 9270.2 MHz)						
- J=1½	-½	½	½	836.76	0.5	5.166
-	½	-½	½	849.68	0.5	5.166
-	1½	½	-½	861.75	0.1	5.166
-	-½	-1½	½	862.34	0.0	5.166
-	½	-½	-½	874.02	-0.8	5.166
-	-½	-1½	-½	885.98	-0.7	5.166
+ J=2½	-1½	-2½	½	1979.49	-0.3	0.085
+	-1½	-2½	-½	2004.22	-0.8	0.085
+	-½	-1½	½	2033.06	2.5	0.085
+	-½	-1½	-½	2058.18	1.7	0.085
+	½	-½	½	2112.92	-2.9	0.085
+	½	-½	-½	2138.24	-3.0	0.085

TABLE III

Fit of the Zero Field Transition Frequencies

Lower state parity	J'	F'	J	F	Observed (MHz)	$\nu_{obs}-\nu_{calc}$ (MHz)	Weight [a] (MHz^{-2})
Microwave spectrum: F_1							
+	1½	2	½	1	124001.566[b]	0.004	400
+	1½	1	½	0	124185.447	-0.007	400
+	1½	1	½	1	124217.490	-0.034	400
-	1½	2	½	1	124309.999	0.031	400
-	1½	1	½	0	124708.812	-0.036	400
-	1½	1	½	1	123682.520	-0.043	400
-	2½	3	1½	2	206850.486	-0.047	400
-	2½	2	1½	1	206899.442	-0.034	400
+	2½	3	1½	2	207127.411	0.044	400
+	2½	2	1½	1	207207.496	-0.022	400
+	3½	3	2½	2	289698.336	0.023	200
-	3½	4	2½	3	289941.435	0.097	400
-	3½	3	2½	2	289974.536	-0.084	400
Microwave spectrum: F_2							
-	2½	3	1½	2	214874.390[b]	0.039	400
-	2½	2	1½	1	215071.199	0.062	400
+	2½	3	1½	2	214877.063	-0.034	400
+	2½	2	1½	1	215072.392	-0.090	400
+	3½	4	2½	3	300831.489	0.042	133
+	3½	3	2½	2	300926.272	-0.15	133
-	3½	4	2½	3	300836.491	-0.051	200
-	3½	3	2½	2	300929.490	-0.096	200
Far infrared rotational spectrum: F_1							
+	9½	9	8½	8	786742.7[c]	-1.5	1.56
+	9½	10	8½	9	786745.8	-1.2	1.56
-	9½	10	8½	9	786974.1	-0.6	1.56
-	9½	9	8½	8	786976.6	-0.3	1.56
-	10½	10	9½	9	869612.7	-0.6	1.56
-	10½	11	9½	10	869616.7	-0.04	1.56
+	10½	10	9½	9	869840.0	1.6	1.56
+	10½	11	9½	10	869840.0	-0.09	1.56
+	11½	11	10½	10	952484.6	-0.3	1.56
+	11½	12	10½	11	952488.7	-0.07	1.56
-	11½	11	10½	10	952705.8	0.1	1.56
-	11½	12	10½	11	952705.8	1.5	1.56
-	12½	12	11½	11	1035354.2	-1.2	1.56
-	12½	13	11½	12	1035359.0	-0.6	1.56
+	12½	12	11½	11	1035569.9	-0.2	1.56
+	12½	13	11½	12	1035569.9	1.0	
Far infrared rotational spectrum: F_2							
+	9½	10	8½	9	815230.5[c]	-0.3	1.56
+	9½	9	8½	8	815248.4	-0.2	1.56
-	9½	10	8½	9	815261.0	0.1	1.56
-	9½	9	8½	8	815274.3	0.09	1.56
-	10½	11	9½	10	900671.8	-0.4	1.56
-	10½	10	9½	9	900687.3	-0.7	1.56
+	10½	11	9½	10	900708.2	0.6	1.56
+	10½	10	9½	9	900719.1	0.5	1.56
-	12½	13	11½	12	1071239.7	-1.1	1.56
-	12½	12	11½	11	1071252.2	-1.5	1.56
+	12½	13	11½	12	1071287.9	0.5	1.56
+	12½	12	11½	11	1071294.9	-0.2	1.56

[a] See text for a discussion of the weights.

[b] Measurements taken from ref. (5).

[c] Measurements taken from ref. (6).

the zero field data. The parameter values determined in the process are given in Table IV. The overall standard deviation of fit relative to the experimental uncertainty was 1.434, a figure which can be regarded as satisfactory. The qualities of the fits of the LMR and EPR data were as expected from the experimental uncertainties. Indeed, the quality of fit of the 635.4-μm spectrum was better than that previously published (*7*). However, neither set of zero field data was fitted quite as well as expected from the authors' estimates of experimental error (*5, 6*).

4. DISCUSSION

The analysis of the available data for CF in the $v = 0$ level has permitted the determination of all its major molecular parameters. The main result from the

TABLE IV

Values (in MHz) for the Molecular Parameters of CF in the $v = 0$ Level of the $X^2\Pi$ State, Derived from a Least-Squares Fit of the Data

$\tilde{A} + \tilde{\gamma}$	2314305.33 (42)[a]	A_D	0.0[b]
$\tilde{\gamma}$	147.69 (17)	$10^2\gamma_D$	-0.44 (23)
B	42197.0591 (48)	10^9H	-0.73[b]
D	0.198748 (44)		
$p + 2q$	257.431 (51)	$10^2(p_D + 2q_D)$	-0.59(18)
q	0.724 (36)	10^4q_D	-0.136[b]
$h_{\frac{1}{2}}$	747.56 (11)	b	268.4 (14)
$h_{\frac{3}{2}}$	664.32 (25)	d	792.195 (98)
g_L'	0.999751 (64)	g_S	2.00196[b]
10^2g_l	0.643 (82)	10^3g_r	-0.215 (30)
$10^2(g_l' - g_r{}^{e'})$	0.3050[b]	$10^4g_r{}^{e'}$	-0.172[b]
g_N	5.2546[b]		
	Derived parameters		
$\tilde{A}$	2314157.64 (45)	p	255.983 (88)
a	705.94 (14)	b_F	151.19 (49)
c	-351.6 (14)		

[a] The numbers in parentheses represent 1 standard deviation of the least-squares fit, in units of the last quoted decimal place.

[b] Parameter constrained to this value in the least-squares fit.

present study is a considerable improvement in the value for the spin-orbit splitting, $(\tilde{A} + \tilde{\gamma})$, to 2314.30533 ± 0.00042 GHz or 77.196916 ± 0.000014 cm^{-1}. The best previous value, determined from an analysis of the optical spectrum (*3*), was 77.11 ± 0.03 cm^{-1}; it can now be seen that the uncertainty quoted was an underestimate. All previous analyses of different parts of the CF data set (*4–7*) have used the older value for the spin-orbit coupling constant. This in itself causes small differences in the values of the parameters determined when compared with those obtained in the present work (Table IV). There are two other features of our Hamiltonian which lead to slightly different parameter values. First, we have used an $\mathbf{N}^2$ formulation whereas others have used an $\mathbf{R}^2$ formulation. The only significant effect of this difference is on the B value determined:

$$B(\mathbf{N}^2) = B(\mathbf{R}^2) + 2D(\mathbf{R}^2). \tag{5}$$

Second, we have constrained A_D to zero in our fits and varied γ whereas most previous studies have adopted the opposite approach. This also causes small differences in the $\tilde{A}$, $\tilde{p}$, and $\tilde{q}$ values (*17, 18*). When all these differences are taken into account, the parameters quoted in Table IV are in good agreement with the values determined previously, particularly those from the analysis of the microwave spectrum (*5*). This is not really surprising since the data sets used have quite large sections in common.

It can be seen from Table IV that three of the six possible g factors have been determined in our work. The orbital g factor differs from unity by $-(2.5 \pm 0.6) \times 10^{-4}$ and is in reasonably good agreement with the relativistic correction to g_L which has been estimated to be -1.8×10^{-4} (*7*). The nonadiabatic correction to g_L (*19*) therefore appears to be insignificant in the case of CF. The rotational g factor, g_r, is determined to be $-0.215(30) \times 10^{-3}$. This value is also in good agreement with the previous estimate of -0.20×10^{-3} (*7*), although this must be somewhat fortuitous since the calculation uses a pure precession model which is unlikely to be valid for CF. The third g factor determined in the fit is g_l, the anisotropic correction to the electron spin g factor. In this case, the value obtained of $0.643(82) \times 10^{-2}$ disagrees markedly with the expectations of the Curl relationship (*20*):

$$g_l = -\gamma/2B \tag{6}$$

which gives a value of -0.175×10^{-2}. We have some confidence in the experimentally determined value since it improves the quality of the fit significantly, particularly for the far-infrared zero field data, and it corresponds to a value of $(p_D + 2q_D)$ which is closer to the value of -0.243×10^{-2} MHz predicted from the formula (*21*):

$$p_D + 2q_D = -2D(p + 2q)/B. \tag{7}$$

A possible explanation for this apparent breakdown of Curl's relationship is that it requires the proper spin–rotation parameter γ (*17*) whereas what has been determined in the fit is only the effective parameter $\tilde{\gamma}$, with the effect of the A_D term absorbed:

$$\tilde{\gamma} = \gamma - A_D(A - 2B)/2B. \tag{8}$$

It has been pointed out elsewhere (*22*) that the parameter $\tilde{g}_l$ is also affected by the constraint of A_D to zero:

$$\tilde{g}_l = g_l - \tfrac{1}{2} g_L A_D/B. \tag{9}$$

If we assume Curl's relationship (*20*) to be valid, we can use it with Eqs. (8) and (9) to determine separate values for A_D and γ:

$$A_D = -(\tilde{\gamma} + 2B\tilde{g}_l)2B/A. \tag{10}$$

Substituting values from Table IV, we obtain

$$A_D = -25 \text{ MHz}, \qquad \gamma = -517 \text{ MHz}, \qquad \text{and} \qquad g_l = 0.00613.$$

These values should not be taken too seriously since several assumptions are involved in their determination. Nevertheless, they are not unreasonable and provide a plausible explanation of the value determined for $\tilde{g}_l$.

Finally, we consider briefly the implications of the ^{19}F magnetic hyperfine parameters. It has only recently been possible to determine all four parameters for CF (*5*). A comparison of the present values with all previous determinations is given in Table V, including the results of an ab initio calculation (*23*). It can be seen that, although $h_{3/2}$ has been reliably determined from the very earliest study by EPR (*4*), the values for the other parameters have varied rather widely until the recent work of Saito *et al.* (*5*). This is because all the earlier determinations depended to a greater or lesser extent on assumed values for one or more of the parameters and the basis for estimation of these assumed values was unreliable. The ab initio calculation by Hall and Richards (*23*) uses restricted Hartree-Fock wavefunctions to estimate the hyperfine parameters. Since this confines the unpaired electron to a π molecular orbital, it provides a particularly poor estimate of the Fermi contact parameter b_F which must necessarily equal zero in this case. However, the estimates for the dipolar and nuclear spin orbit coupling parameters are not too bad as can be seen from Table V. Kristiansen and Veseth (*24*) have recently shown that it is now possible to compute hyperfine parameters with an accuracy of a few percent.

TABLE V

A Comparison of Various Determinations of the Nuclear Hyperfine Parameters for CF in Its $X^2\Pi$ State

Parameter (MHz)	Present work	Saito et al. (5)	Van den Heuvel et al. (6)	Saykally et al. (7)	Carrington and Howard (4)	Hall and Richards (23)
$h_{\frac{3}{2}}$	664.31(25)	664.07(23)	663.5(30)	665.7(83)	662.9(30)	522
$h_{\frac{1}{2}}$	747.56(11)	747.58(10)				
a	705.94(14)	705.82(16)	633(29)	698 [a]		628
b	268.4(14)	269.2(14)	261(6)	253(22)	190(50)	106
b_F	151.19(49)		195(18) [b]	147 [a]		0
c	-351.6(14)	-352.7(17)	-200(61) [b]	-318 [c]		-318
d	792.195(98)	792.17(9)	772(27)	782(309)		

[a] Error not quoted by the authors.

[b] Calculated value.

[c] Value taken from Hall and Richards (*23*).

TABLE VI

^{19}F Hyperfine Structure Parameters (in m^{-3})

Expectation value	CF	F [a]
$\langle r_i^{-3} \rangle_\ell$	9.502×10^{30}	4.96×10^{31}
$\psi(0)^2$	0.2429×10^{30}	0.484×10^{30}
$\langle (3\cos^2\theta_i - 1)/r_i^3 \rangle_s$	-3.151×10^{30}	
$\langle \sin^2\theta_i / r_i^3 \rangle_s$	7.100×10^{30}	
$\langle r_i^{-3} \rangle_s$	9.075×10^{30}	5.49×10^{31}

[a] From Harvey (*25*).

The ^{19}F hyperfine parameters determined in the fit can be related quite simply to expectation values of distribution functions over the electronic wavefunction. The results obtained are given in Table VI, together with the corresponding values for atomic fluorine (*25*) for comparison. The interpretation of these quantities has already been discussed quite thoroughly by Saito *et al.* (*5*) and we shall not repeat them here. There are a couple of additional points of interest. Although the orbital average $\langle r_i^{-3} \rangle_l$ is close to the spin average, it is nonetheless significantly different from it, reflecting the fact that the orbital and spin angular momenta are not carried by exactly the same electrons in CF. It is interesting to note in this case that the orbital average is about 5% larger than the spin average, whereas for the atom it is about 10% smaller. From the Fermi contact interaction, the unpaired electron density at the ^{19}F nucleus of CF is determined to be about half the value in atomic fluorine. However, since the spin density on the F atom, as determined from the dipolar interaction, is 0.18, the spin polarization effects are actually greater in CF than in atomic fluorine.

In this work, we have been able to measure the last outstanding major parameter for CF in its ground electronic state. Results from previous studies of this molecule have been drawn together to provide the best available set of parameters and all of its primary structural characteristics have now been determined.

ACKNOWLEDGMENT

We are grateful to the Science and Engineering Research Council for the support of one of us (J.E.S.).

RECEIVED: June 24, 1986

REFERENCES

1. E. B. ANDREWS AND R. F. BARROW, *Nature (London)* **165,** 890 (1950).
2. E. B. ANDREWS AND R. F. BARROW, *Proc. Phys. Soc. London Sect. A* **64,** 481–492 (1951).

3. T. L. PORTER, D. E. MANN, AND N. E. AQUISTA, *J. Mol. Spectrosc.* **16,** 228–263 (1965).
4. A. CARRINGTON AND B. J. HOWARD, *Mol. Phys.* **18,** 225–231 (1970).
5. S. SAITO, Y. ENDO, M. TAKAMI, AND E. HIROTA, *J. Chem. Phys.* **78,** 116–120 (1983).
6. F. C. VAN DEN HEUVEL, W. L. MEERTS, AND A. DYMANUS, *Chem. Phys. Lett.* **88,** 59–62 (1982).
7. R. J. SAYKALLY, K. G. LUBIC, A. SCALABRIN, AND K. M. EVENSON, *J. Chem. Phys.* **77,** 58–67 (1982).
8. K. KAWAGUCHI, C. YAMADA, Y. HAMADA, AND E. HIROTA, *J. Mol. Spectrosc.* **86,** 136–142 (1981).
9. M. A. GONDAL, W. ROHRBECK, W. URBAN, R. BLANCKART, AND J. M. BROWN, *J. Mol. Spectrosc.* **100,** 290–302 (1983).
10. J. M. BROWN, A. R. H. COLE, AND F. R. HONEY, *Mol. Phys.* **23,** 287–295 (1972).
11. M. MIZUSHIMA, K. M. EVENSON, AND J. S. WELLS. *Phys. Rev. A* **5,** 2276–2287 (1972).
12. J. M. BROWN, A. CARRINGTON, AND T. J. SEARS, *Mol. Phys.* **37,** 1837–1848 (1979).
13. T. J. SEARS, P. R. BUNKER, A. R. W. MCKELLAR, K. M. EVENSON, D. A. JENNINGS, AND J. M. BROWN, *J. Chem. Phys.* **77,** 5348–5362 (1982).
14. J. M. BROWN, C. M. L. KERR, F. D. WAYNE, K. M. EVENSON, AND H. E. RADFORD, *J. Mol. Spectrosc.* **86,** 544–554 (1981).
15. J. E. SCHUBERT, Ph.D. thesis, Southampton University, 1984.
16. J. M. BROWN, E. A. COLBOURN, J. K. G. WATSON, AND F. D. WAYNE, *J. Mol. Spectrosc.* **74,** 294–318 (1979).
17. J. M. BROWN AND J. K. G. WATSON, *J. Mol. Spectrosc.* **65,** 65–74 (1977).
18. J. M. BROWN, J. E. SCHUBERT, C. E. BROWN, J. S. GEIGER, AND D. R. SMITH, *J. Mol. Spectrosc.* **114,** 185–196 (1985).
19. J. M. BROWN AND H. UEHARA, *Mol. Phys.* **24,** 1169–1174 (1972).
20. R. F. CURL, *Mol. Phys.* **9,** 585–597 (1965).
21. L. VESETH, *J. Phys. B.* **3,** 1677–1691 (1970).
22. K. M. EVENSON, R. J. SAYKALLY, D. A. JENNINGS, R. F. CURL, AND J. M. BROWN, "Chemical and Biochemical Applications of Lasers" (C. Bradley Moore, Ed.), Vol. 5, pp. 95–138, 1980.
23. J. A. HALL AND W. G. RICHARDS, *Mol. Phys.* **23,** 331–343 (1972).
24. P. KRISTIANSEN AND L. VESETH, *J. Chem. Phys.* **84,** 6336–6344 (1986).
25. J. S. M. HARVEY, *Proc. R. Soc. London, Ser. A* **285,** 581–596 (1965).
26. M. INGUSCIO, G. MORUZZI, K. M. EVENSON, AND D. A. JENNINGS, *Rev. Appl. Phys.* (in press).